The Scattering of Protons by Protons from 200 to 300 kev

G. L. RAGAN,* W. R. KANNE,** AND R. F. TASCHEK‡
University of Wisconsin, Madison, Wisconsin

(Received September 2, 1941)

Proton-proton scattering between 200 and 300 kev has been studied as a function of energy and of angle. The results are in good agreement with Breit's calculations based on a square well proton-proton interaction potential of e^2/mc^2 radius and 10.500 Mev depth. The scattering chamber was isolated from the accelerating tube by a differential pumping system. Scattered protons were detected by Geiger-Klemperer proportional counters filled with purified hydrogen. Two separate counters connected to similar amplifier-recorder circuits detected simultaneously protons scattered at different angles from the beam, and the ratio of scattering at these angles was calculated directly. Tests of the performance of the counters are given. Two different scattering chambers yielded similar results.

INTRODUCTION

EXPERIMENTS performed in 1936 by Tuve, Heydenburg, and Hafstad[1] on protons of 600- to 900-kev energy scattered by hydrogen gave results differing greatly from that predicted by Mott's formula which is based on a repulsive Coulomb field between protons. A mathematical analysis by Breit, Condon, and Present[2] showed that these data were best explained by assuming the presence of an attractive nuclear force between protons at small separations. These analyses indicated that a minimum in the 45° scattering should occur in the neighborhood of 400 kev, because of the interference between the repulsive Coulomb scattering and the attractive nuclear force scattering. In 1937 Hafstad, Heydenburg, and Tuve,[3] using protons of 200 to 600 kev, found proof of the existence of this minimum.

Accurate scattering data enable one to determine the width, r_0, and the depth, D, of the square potential well representing the interaction between protons. The high energy data[4, 5] analyzed by Breit, Thaxton, and Eisenbud[6] (hereafter referred to as BTE) indicate good agreement with a well of radius e^2/mc^2 and depth 10.500 Mev. A well of $0.75e^2/mc^2$ radius and 19.6905-Mev depth gives the same scattering at 2200-kev energy (see Fig. 7 of BTE), so that either well may be considered as fitting the data at the highest voltages investigated. However, the theoretical scattering curve for the 19.6905-Mev well deviates from the experimental points at lower voltages.

The desirability of obtaining accurate data in the low energy region was pointed out by BTE, pp. 1057–1060. On either side of the above-mentioned minimum the scattering is particularly sensitive to the choice of well parameters, hence experiments at about 300 kev and at about 500 kev are particularly good for determining these. The principal object of the experiments reported in this paper is to obtain data at energies below that at which the scattering minimum occurs, of sufficient accuracy to enable a clear choice to be made between the two wells mentioned above.

SCATTERING CHAMBERS

Two different scattering chambers were used. The first was one having fixed openings at 15° intervals into which counters could be waxed. These openings were in the form of accurately aligned tubes; the defining slits and holes of the counters were centered in tubes which slipped

* Now at Massachusetts Institute of Technology.
** Now at Illinois Institute of Technology.
‡ Now at Oldbury Electro-Chemical Company, Niagara Falls, New York.
[1] M. A. Tuve, N. P. Heydenburg, and L. R. Hafstad, Phys. Rev. **50**, 806 (1936).
[2] G. Breit, E. U. Condon, and R. D. Present, Phys. Rev. **50**, 825 (1936).
[3] L. R. Hafstad, N. P. Heydenburg, and M. A. Tuve, Phys. Rev. **53**, 239 (1938).
[4] R. G. Herb, D. W. Kerst, D. B. Parkinson, and G. J. Plain, Phys. Rev. **55**, 998 (1939).
[5] N. P. Heydenburg, L. R. Hafstad, and M. A. Tuve, Phys. Rev. **56**, 1078 (1939).
[6] G. Breit, H. M. Thaxton, and L. Eisenbud, Phys. Rev. **55**, 1018 (1939).

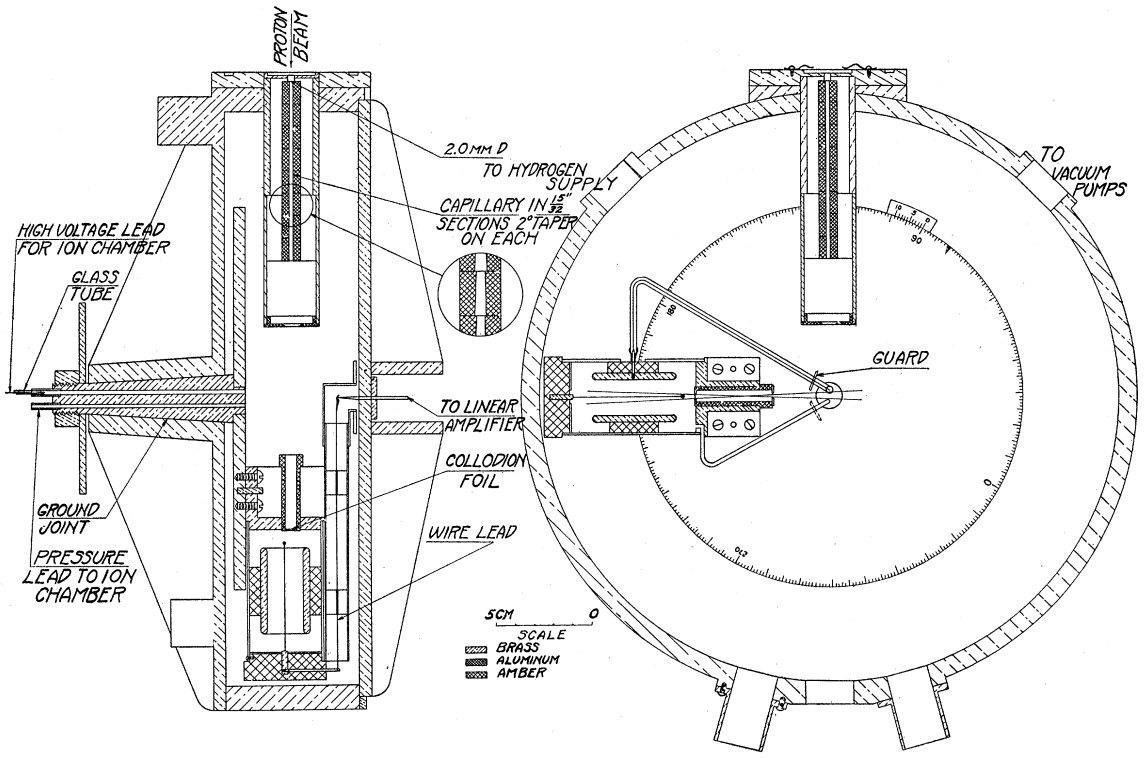

FIG. 1. Scattering chamber, referred to as the second chamber.

snugly into these. This was the same apparatus shown in Fig. 3 of an earlier paper[7] from this laboratory, with the exception of the counting apparatus. Only four of the 15°-interval tubes are shown there; actually there were openings at 15°, 30°, 45°, 60°, 75°, and 105°, both right and left of the beam. Four counters were used at angles 15° left, 30° left, 15° right, and 45° right in taking the hydrogen data. Two similar pulse amplifiers were used, enabling us to count simultaneously at two angles. The openings of the defining systems were made of such size that comparable counting rates occurred at various angles.

The second scattering chamber was more versatile than the first one. It has only two openings of the aligned-tube type; these were at 15°, right and left, and into them two monitoring counters were fitted. These were ordinarily connected in parallel to the same amplifying circuit in order to reduce errors due to possible fluctuations of beam position. A third counter, with larger defining apertures was mounted inside the scattering chamber on a graduated disk which could be rotated by means of a ground joint. At angles smaller than 35°, the rotating counter obstructed the monitor on its own side of the beam, so only the one on the opposite side of the beam was used. Correspondingly, the beam itself struck the body of the counter at angles below 22°. No effect attributable to this was observed when the scattering chamber was evacuated. Two views of the complete chamber are given in Fig. 1. Apiezon grease *N* was used on the ground joint. The top plate was waxed on with Picein wax; the two monitor counters were also waxed in with Picein into the two aligned tubes shown at 15° in Fig. 1. The body of the chamber and the top plate were turned from brass castings. The guard shown near the center of the chamber occupied the dashed position when the counter was on the right side of the chamber. It was useful at smaller angles to protect the defining slit system of the rotating counter from slit scatter-

[7] W. R. Kanne, R. F. Taschek, and G. L. Ragan, Phys. Rev. **58**, 693 (1940).

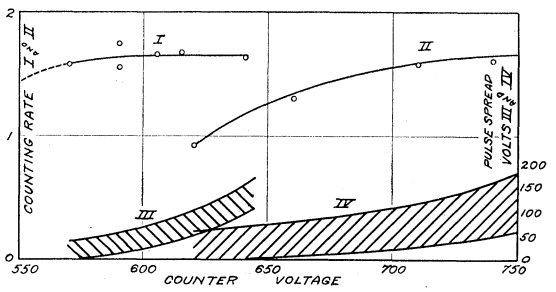

FIG. 2. Proportional counter plateaus and corresponding pulse spreads. Pulse spreads were visually estimated on oscilloscope on output of linear amplifier. These data were taken at 250 kv with protons scattered at 45° in hydrogen. The counter contained hydrogen at 25 mm of mercury pressure for curves I and III, and 44-mm pressure for curves II and IV.

ing from the collimating capillary system; this guard, as well as the general design of the apparatus, was similar to that of Herb and collaborators.[4] Along with the diaphragm shown about halfway between the exit end of the collimating capillary and the center of the chamber, it gave adequate protection against slit scattering.

COUNTERS

There are several difficulties which arise in the low energy region which are not met with in the higher energy range. The most important of these is that the ionization-collecting counter used at higher energies will not detect a proton of these low energies because of insufficient ionization per proton. Our first problem, then, was to find a reliable detector for protons of 100 to 150 kev, since these are the energies of protons scattered at 45° from a beam of 200 to 300 kev. In their experiments in this region, Hafstad, Heydenburg and Tuve[3] used Geiger point counters. These they found to be sensitive, but not quantitatively reliable. We first tried using gross ionization current measured with an Edelmann string electrometer, as described in another paper[7] from this laboratory. This method, however, was not sufficiently sensitive nor quantitative for this problem.

The counters finally adopted were of the Geiger-Klemperer proportional-counter type. Figure 1 includes two views of one of our counters. The rest of our counters were essentially the same, being of the same construction as shown by Brubaker and Pollard,[8] but about twice as long and half as large in diameter as theirs. The defining slit and hole were so placed that the protons detected traveled the entire length of the counter, roughly parallel to the center wire. The wire was connected to the first stage of a five-stage pulse amplifier with reduced gain (three stages would probably have sufficed). The cylinder surrounding the wire was maintained at a constant potential of some 600 to 900 volts negative. The counter was separated from the scattering chamber by a thin foil of collodion, of perhaps 20-kev stopping power; it was filled with purified hydrogen at presures of 3 to 4 cm of mercury. Brubaker and Pollard found hydrogen to be one of the best gases tried in this type of counter. A further advantage was that any leakage from the counters into the scattering chamber did not contaminate the chamber; this is important as these extremely thin collodion foils always leaked a little.

These counters gave good voltage plateaus, as indicated in Fig. 2. The two counter pressures illustrated are extremes, most of our data having been taken at pressures of 30 to 40 mm of mercury. The pulse size was visually estimated on a cathode-ray oscilloscope connected to the output of the amplifier. It was always found that if the output pulses were greater than 50 volts and less than 120 volts the counters were operating in the plateau region. This afforded a convenient means of setting counter voltages. It will be noticed that the pulse distribution as well as the plateau was better in the case of the 25-mm curve. This was true only for low proton energies, and may probably be given the following explanation. Let us assume a reasonable range of energies to be present in the protons entering the counter, this spread being due to straggling in the collodion foil, variation in thickness of foil passed through due to curvature of the foil under gas pressure, variations in loss of energy in the gas of the scattering chamber, etc. If the gas pressure in the counter is low enough so that all the protons have residual ranges greater than the counter length, then the differences in pulse size will presumably be due to variations in specific ionization alone. However, if the gas

[8] G. Brubaker and E. Pollard, Rev. Sci. Inst. **8**, 254 (1937).

pressure is high enough that a considerable number of the protons are stopped in the counter, then the variation in total ionization over these residual ranges will enter. On the other hand, too low a counter pressure gave poor plateaus for protons of any energy used. Pressures of about 30 to 40 mm of mercury seemed to be quite satisfactory in all respects.

As a further check on the performance of the counters, the scattering of protons in purified helium at 105° and 60° was observed with the first chamber by counting simultaneously at these angles with two separate counters. The same two counters were used as were used at 45° and 30° in the hydrogen work with the first chamber. The energies of the protons scattered at these angles in helium are 52.5 percent and 77.0 percent of the beam energy, which is almost the same as the 50.0 percent and 75.0 percent for 45° and 30° in hydrogen. Figure 3 shows the results. Vertical lines on the points indicate their statistical reliability. The horizontal line at 15.15 $\times 10^{-2}$ is the value of the scattering ratio given by Rutherford's formula which is probably valid under these conditions. Experiments at the Carnegie Institution of Washington[9] on proton-helium scattering show an anomaly at 1 Mev which increases with both energy and angle, and indicates that too much faith should not be placed in this assumption. However, the fact that our proton-helium scattering ratio agrees so well with the Rutherford formula at 300 kev, where it is expected that our counters should be quite reliable, seems to argue against the presence of any appreciable anomaly under the conditions of our experiment. The fact that the observed ratios are less than the Rutherford value below 300 kv is just what is to be expected on the basis of our observations of the counter behavior. At 200 kv and below it was obvious from oscilloscopic observations of the pulses that the spread in pulse size was excessive, and that a considerable percentage of them were not large enough to be recorded by the recording circuit. This situation gradually improves with increasing beam energy, so that the efficiency of the counters should approach unity at higher energies. Thus it seems quite safe to assume (1) that there is no detectable scattering anomaly at 105° for a beam energy of 300 kev and (2) that the low values observed for the 105°/60° ratio are caused by reduced efficiency of the counters. On the basis of these assumptions, the proton-helium scattering ratio curve was used to determine the efficiency of the counters as a function of proton energy. These efficiencies have been used in making corrections to the 45°/30° data in hydrogen given in Fig. 8, taken with the first scattering chamber.

A new counter was constructed for use as the rotating counter in the second scattering chamber, and a separate determination of its efficiency was made. It was convenient to use the results of the 250-kev angular distribution data (Fig. 10) for this purpose. According to the laws of conservation of energy and momentum, in the collision of identical particles equal numbers of particles per unit target volume are scattered into equal angular ranges symmetrical with respect to 45°. The energy of a particle scattered at a small angle is great and the efficiency of the counter is unity. The scattering yield may then be used to predict an expected Mott ratio for the angle symmetrical with respect to 45°. The Mott ratio observed divided by that expected at an angle above 45° gives directly the efficiency of the counter for an incoming particle of the energy corresponding to that angle. The energy of a scattered proton is given by the beam energy multiplied by the square of the cosine of the scattering angle. Figure 4 gives the efficiency of

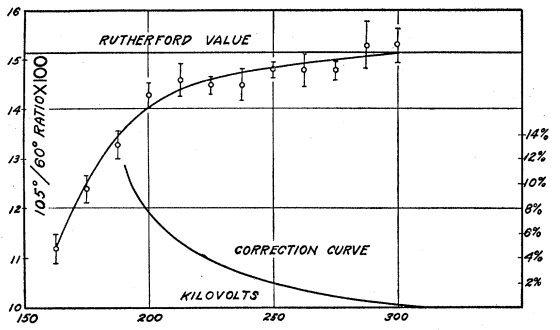

FIG. 3. Counter efficiency correction curve applying to 45°/30° ratio data of first chamber, Fig. 8. The experimental points give the ratio of 105° to 60° scattering of protons in helium. The lower curve and right hand ordinate scale give the efficiency correction. The abscissa refers to accelerating tube voltage.

[9] N. P. Heydenburg and R. B. Roberts, Phys. Rev. **56**, 1092 (1939); N. P. Heydenburg and N. F. Ramsey, Jr., Phys. Rev. **60**, 42 (1941).

the rotating counter as a function of the energy of incident protons.

Other Apparatus and Techniques

The essential features of the transformer-rectifier high voltage apparatus have been described by Haworth, King, Zahn, and Heydenburg.[10] An approximate calibration of the voltmeter has indicated no disagreement with the original calibration discussed in reference 10, which has been used in this work. The high voltage ripple was 1 percent r.m.s.

The proton beam entered the second chamber through a $3\frac{3}{4}$-inch capillary tube of 2 mm diameter; it was made up of eight sections, each tapered 2° to prevent any of the beam striking the wall of the capillary and being scattered with reduced energy into the chamber along with the true beam. The first chamber had a similar 3-inch capillary of six sections. The proton beam did not pass through any foil in entering the chamber. There was a continual flow of hydrogen into the chamber and through the capillary, thereby maintaining pressures up to 1 or 2 mm of mercury. This pressure was measured by a manometer containing low vapor pressure diffusion pump oil. A differential pumping system then removed the gas, isolating the scattering chamber from the vacuum maintained in the accelerating tube. This pumping apparatus and capillary are described more fully in reference 7. In some early trials using thin aluminum foils to isolate the chamber we found by magnetic analysis that much energy straggling was introduced by passing the beam through such a foil. This difficulty is, of course, of little moment at the beam energies used by others in the high energy region. The fact that fresh gas was continually being supplied and contamination swept out was also advantageous.

Rather than trying to measure the actual beam current (0.1 to 0.2 microampere came through the differential pumping channels and capillary) we adopted the procedure of counting scattered protons simultaneously at two different angles. This gave directly the ratio of the scattering at these two angles, provided the geometry of the counters was known. Or, one angle could be used simply for a monitor, and the other counter could be set at different positions; this gave for each angle the count relative to that at the monitor position. These methods have the following desirable features. (1) They eliminate the need for current measurement. Such a measurement would be exceedingly difficult to make accurately since capture and loss of electrons by protons of the beam would be appreciable in passing through a foil into a Faraday cage, or even in passing through the gas of the chamber itself. (2) Accurate pressure measurement and control are unnecessary, since pressure changes affect both counters similarly. (3) A certain amount of voltage fluctuation is compensated for; for instance, the ratio of the counts at a given pair of angles would remain constant at all energies for Rutherford scattering.

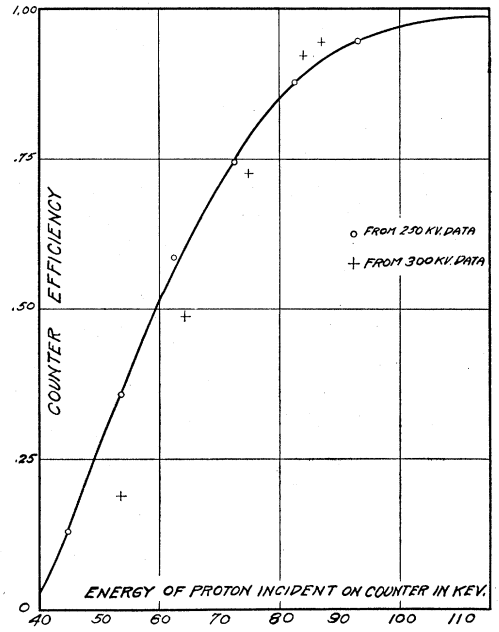

FIG. 4. Efficiency of rotating counter in second scattering chamber. The 250-kv data are the more reliable and are used as the basis for the correction.

To assure that the proton beam accurately intersected the axis of the scattering chamber, the chamber was shifted until the proton-beam spot fell near the center of a quartz plate at the end of the scattering chamber. Since it was necessary for the beam to traverse the 2-mm capillary of the differential pumping system with as little loss of current as possible, leveling screws

[10] L. J. Haworth, L. D. P. King, C. T. Zahn, and N. P. Heydenburg, Rev. Sci. Inst. 8, 486 (1937).

moving the chamber in and perpendicular to its plane were next used to adjust the chamber to the position where maximum current was obtained in a Faraday cage at the end of the (evacuated) scattering chamber. This procedure was followed with both chambers.

To further center the beam in the second chamber, the rotating counter was set at 45° where the scattering varied slowly with angle, and the chamber was adjusted until the ratio of the scattering into the left monitor to the scattering into the 45° counter was equal to the same ratio for the right monitor. The slightly different geometrical apertures of the two monitor counters were of course allowed for.

To determine the exact zero of the divided circle, the ratio of the scattering at 250 kev at angles 35°, 36°, 37.5° and 39° to that at 15° was taken with the rotating counter first on one side of the beam, then at the corresponding angles on the other side. These data were plotted separately, each set being accurately linear and quite parallel but differing from the other by an angular displacement of 0.8°. It was then assumed that the zero of the scale was off by 0.4° and all the data shown were taken at the correct angles.

Observations have been taken in the angular range 15° to 90° to determine whether any large amount of slit scattering was present with the scattering chamber evacuated. Too few pulses from the monitors were observed on the oscilloscope to allow counting, but quite a few pulses from the rotating counter were observed for angles below about 25°. Since there was gas leakage from the counters which were at a pressure of 45 mm of mercury, and since the geometry factor for the rotating counter was about ninety times that of either of the monitors, the number of pulses at small angles was no more than was to be expected on the basis of scattering from residual gas in the chamber. These observations were made at both 250 kv and 300 kv, with the number of pulses observed with the rotating counter at small angles being appreciably less at the higher voltage. There is, of course, the possibility that there still are slit scattering effects in the proton-proton scattering data due to the spreading of the beam when gas is in the chamber, but the effect of this spreading cannot easily be estimated, and can hardly be large.

The counting circuit was so arranged that the two recording circuits and a clock were turned on and off simultaneously. The time was, of course, not directly needed in the calculations, but gave a useful check of counting rates. During the taking of the data frequent checks were made on the character of pulses and background by observation with a cathode-ray oscilloscope which could be switched from one counting circuit to another. With each change in energy or angle the counter voltages had to be re-set, since the size of pulse was proportional to the ionization produced by the proton. As mentioned above, when discussing counters, the proper voltage was easily and reliably determined by setting for pulses in the range of 50 to 120 volts at the amplifier output. During the course of a run the pressure in the counters slowly decreased due to leakage through the foils; this also necessitated counter voltage adjustment several times an hour.

Before starting a run the counters were filled with fresh hydrogen, purified by passage through a palladium tube. Then this same hydrogen source was used to furnish the gas for the scattering chamber; as mentioned above, this gas was continuously admitted and pumped out through the capillary. Liquid air was supplied to a trap which had large diameter connections with the scattering chamber.

Reduction of the Data

Since the data were taken as the ratio of the scattering at two angles, it was necessary to know the relative geometrical factors involved in the counters being used. Table I gives the various dimensions of all the counters used in the data reported herein. The notation is that of BTE, reference 6.

At the beginning and end of each run, and sometimes in between, a check was made of the contamination in the following way. The beam voltage was set at 100 or 150 kv, and the 45° counter voltage so adjusted that the protons scattered from hydrogen, having lost half their energy in the collision, were not detected, while those scattered from heavier contaminant atoms, having lost little energy, gave large enough pulses to be counted reliably. Thus the 45° counter registered only the scattering due to contaminants. When counting was done at the same time

at an angle of either 15° or 30°, no separation of these two scattered groups occurred, since little energy was lost in either type of collision. From a comparison of the contaminant scattering (45°) with contaminant plus hydrogen scattering (15° or 30°), the amount of contamination present was calculated. Since our data seemed from the outset to be in approximate agreement with the calculations of BTE for an interaction well of e^2/mc^2 radius and 10.500-Mev depth, the contamination corrections were made by assuming these calculations for the hydrogen scattering and the Rutherford law for contaminant scattering. The amount of contamination present is conveniently expressed in terms of the equivalent air pressure (in units of 10^{-4} mm of mercury per mm of mercury of hydrogen pressure in the scattering chamber) which would give the observed scattering, and is called A/p. Simultaneous counting of course only gives the ratio of contamination to hydrogen. Because of the anomaly, the proton-proton scattering intensity in these experiments is very low, causing this correction to be of considerable importance. The variation of the contamination correction with angle is shown in Figs. 5, 6, and 7.

Another important correction, referred to as the geometry correction, is due to the non-linear variation of scattering with angle. Since the defining slit system for the counters necessarily admits scattering from a finite range of angles, this non-linearity causes the scattering observed to be too great. Corrections for this effect were made on the basis of Eq. (7.2) of BTE, again under the assumption that the scattering follows the calculations for the 10.500-Mev well. Had the 19.6905-Mev well been assumed, the corrected ratio for 45°/30° at 300 kev would have been raised by approximately 3 percent, while at other angles and lower energies the difference between the results with the two wells would be much less. The corrections calculated from Eq. (7.2) of BTE agreed extremely well with earlier calculations made as follows. The hole of the counter defining-system was divided into several zones parallel to the defining slit. Then the area under the theoretical scattering curve between the limits defined by the slit was found for the average angle corresponding to each zone. These curve-areas were weighted according to the corresponding zone-area, and averaged. Comparison of this averaged area with that which would have been obtained had the angular variation been linear gave the desired correction. The variation of the geometrical correction with angle is included in Figs. 5–7.

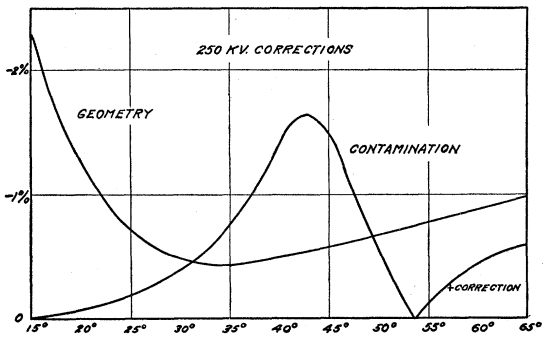

FIG. 5. Geometry and contamination correction curves for the 250-kv data, Fig. 10, and Table III. The contamination correction is for units of A/p, the equivalent air contamination in 10^{-4} mm of mercury per mm of mercury of hydrogen pressure in the scattering chamber.

TABLE I. *Data on counter slit systems. All dimensions are given in millimeters. The notation is that of* BTE, *p. 1026. The geometrical constant of a counter slit system is given by* $2\pi ba^2/R_0h$; *numbers proportional to the various values of this expression are given in the last two columns.*

First or Second Apparatus	Angle	Slit Width "2b"	Hole Diam. "2a"	Hole to Slit "h"	Hole to Center "R_0"	Relative Geometry Factor	
First	45°H_2 105°He	4.042	3.080	40.0	155	36.10	
First	30°H_2 60°He	1.964	1.840	40.0	155	6.250	
First	15°	1.007	1.028	40.0	155	1.000	
First	15°	1.024	1.018	40.0	155	1.000	
Second	15°R	0.106	1.028	40.0	192	0.0852	1.083
Second	15°L	0.100	1.018	40.0	192	0.0787	1.000
Second	Rotates	0.868	2.009	40.0	70	7.30	92.8

It should be recalled that an efficiency correction, described in the section on counters, was applied to the energy variation data. Also, the 300-kv angular distribution data (Fig. 11) were corrected for pick-ups from sparks on the assumption that each spark caused one extra pulse. The inaccuracy of this correction when the counting rate is low indicates that the deviation at 45° may originate in this way.

Discussion of Results

The results of the experiments with the first scattering chamber are summarized in Table II and Figs. 8 and 9. In this table total counts

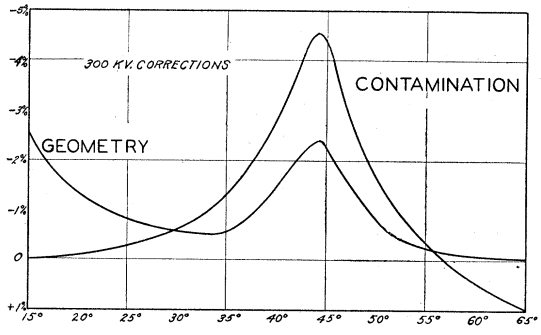

FIG. 6. Geometry and contamination corrections for the 300-kv data, Fig. 11 and Table IV. The contamination corrections are for units of A/p.

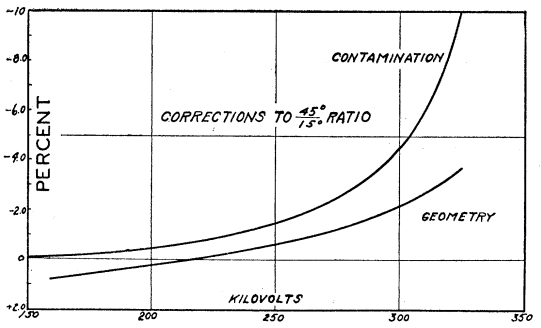

FIG. 7. Geometry and contamination correction curves for the 45°/15° ratio data, Fig. 12 and Table V. The contamination correction is for units of A/p.

representing numerous runs are given. Particular emphasis was placed on the 45°/30° data. These data were broken down into six groups as follows: three ranges of scattering pressure were chosen—5 to 10 mm of oil (density 0.89), 10 to 15 mm, and 15 to 20 mm; in each of these, two subgroups were made by counter pressure, one for pressures below 35 mm of mercury and one for higher pressures. Plotting these points revealed no systematic trend of the data with either counter pressure or scattering pressure variations. The lack of an effect with changing scattering pressure seems to eliminate the possibility of any appreciable errors due to multiple scattering in the data obtained with the first scattering chamber. The data taken at 320 kv are included, though it should be pointed out that the sparking of the outfit, which was not corrected for in this point, the small number of counts, and the geometry and contamination corrections of about 30 percent cast doubt upon the reliability of this point.

Angular distribution data taken with the second scattering chamber for the range from 15° to 65° have been obtained for incident proton energies of 249.5 kev and of 298.3 kev. These data have been expressed in the form of a ratio P/P_M of observed scattering to the scattering expected from Mott's formula, because the scattering at low angles is of a different order of magnitude than that at 45°. The values of P/P_M

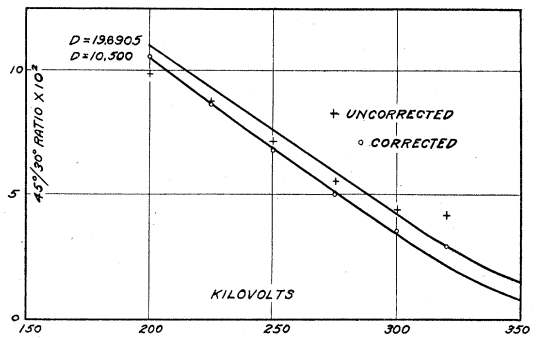

FIG. 8. Proton-proton scattering, first chamber data. The ratio of 45° scattering to 30° scattering multiplied by 100 is plotted as a function of voltage along with the corresponding theoretical curves (solid lines) for $r_0=\frac{3}{4}e^2/mc^2$, $D=19.6905$ Mev and $r_0=e^2/mc^2$, $D=10.500$ Mev.

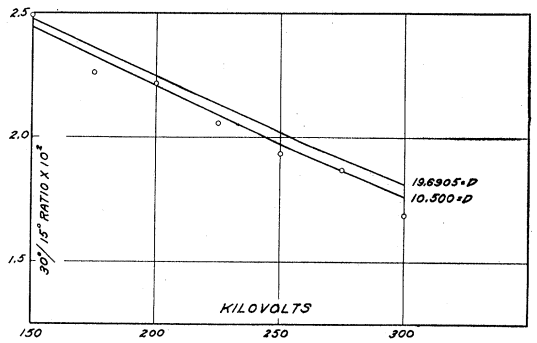

FIG. 9. Proton-proton scattering, first chamber data. The ratio of 30° scattering to 15° scattering multiplied by 100 is plotted as a function of voltage, along with the corresponding theoretical curves (solid lines) for $r_0=\frac{3}{4}e^2/mc^2$, $D=19.6905$ Mev, and also $r_0=e^2/mc^2$, $D=10.500$ Mev.

TABLE II. *Proton-proton scattering results, first apparatus.*

Variation with energy, 45° to 30° ratio						
Energy, kev	200	225	250	275	300	320
Total counts at 45°	29,044	78,284	31,272	12,604	4,864	420
Total counts at 30°	50,960	155,104	75,104	39,248	19,152	1,728
Uncorrected ratio, %	9.88	8.74	7.21	5.56	4.40	4.21
Corrected ratio, %	10.53	8.65	6.80	5.00	3.58	2.99

Variation with energy, 30° to 15° ratio							
Energy, kev	150	175	200	225	250	275	300
Total counts at 30°	12,760	5,028	4,448	15,612	6,668	5,040	4,680
Total counts at 15°	82,048	35,456	31,680	120,096	54,544	42,448	43,472
Uncorrected ratio, %	2.49	2.27	2.25	2.08	1.96	1.90	1.72
Corrected ratio, %	2.49	2.26	2.24	2.06	1.94	1.87	1.69

TABLE III. *Angular variation of P/P_M at 249.5 kev. θ, angle; C, counter and scaling circuit used; N_P, actual number of protons counted; p, hydrogen pressure in scattering chamber in mm of oil; A/p, ratio of equivalent air pressure in units of 10^{-4} mm of mercury giving observed contamination, to chamber pressure in mm of mercury;* Corr, *sum of geometry and contamination corrections in percent; R, observed scattering ratio, including geometrical factor, multiplied by 10^4; $(P/P_M)u$, uncorrected ratio to Mott; $(P/P_M)c$, ratio to Mott with geometry and contamination corrections. The "A" counter is the monitor at 15°, "B" is the rotating counter.*

θ	C	N_P	p	A/p	Corr	R	$(P/P_M)u$	$(P/P_M)c$
15°	A4	776						
	B16	71,100	9.5	2.52	−2.3	10,710	0.952	0.929
345°	A4	840						
	B16	72,600	9.5	2.52	−2.3	9,360		
20°	A4	2,544						
	B16	46,500	11.2	2.64	−1.45	2,140	0.876	0.865
340°	A4	2,500						
	B16	48,850	10.6	2.64	−1.45	2,120		
22.5°	A4	3,628						
	B16	36,020	12.3	1.69	−1.19	1,162	0.845	0.836
337.5°	A4	3,276						
	B16	34,200	12.3	1.69	−1.19	1,130		
25°	A4	1,468						
	B16	7,610	7.2	4.0	−1.50	607		
25°	A4	3,312						
	B16	16,910	11.4	2.5	−1.20	598	0.781	0.769
335°	A4	1,672						
	B16	9,060	7.1	4.0	−1.50	587		
335°	A4	2,400						
	B16	13,200	11.2	2.5	−1.20	596		
27.5°	A4	1,544						
	B16	4,530	7.2	4.0	−1.68	343		
27.5°	A4	2,868						
	B16	8,565	11.2	2.5	−1.26	337	0.734	0.723
332.5°	A4	1,568						
	B16	4,965	7.2	4.0	−1.68	342.5		
332.5°	A4	3,516						
	B16	10,920	11.1	2.5	−1.26	337		
30°	A4	1,880						
	B16	3,360	7.2	3.95	−2.08	209		
30°	A4	3,516						
	B16	6,080	10.2	3.0	−1.70	202	0.681	0.674
330°	A4	3,444						
	B16	6,320	10.1	3.0	−1.70	199		
330°	A4	1,848						
	B16	3,441	7.2	3.95	−2.08	201.7		
32.5°	A4	2,512						
	B16	2,674	7.2	3.95	−2.51	124.3	0.624	0.606
327.5°	A4	2,024						
	B16	2,207	7.2	3.95	−2.51	118.1		
35°	A4	6,098						
	B16	3,600	11.2	2.0	−1.97	69.2		
35°	A16	5,165						
	B4	1,604	7.0	3.95	−3.47	69.6	0.524	0.506
325°	A16	4,148						
	B4	1,428	7.2	3.95	−3.47	77.3		
325°	A16	5,860						
	B4	3,516	11.2	2.0	−1.97	65.0		
37.5°	A16	7,655						
	B4	1,424	7.1	4.20	−4.75	41.75	0.421	0.401
322.5°	A16	7,945						
	B4	1,412	7.1	4.20	−4.75	39.87		
40°	A16	11,200						
	B4	1,328	7.1	3.95	−6.03	26.53	0.348	0.335
320°	A16	16,770						
	B4	1,848	23.5	1.13	−2.08	24.75		
42.5°	A16	16,490						
	B4	1,296	7.0	3.95	−7.04	17.65		
42.5°	A16	24,590						
	B4	1,924	21.4	1.10	−2.34	17.51	0.286	0.275
317.5°	A16	29,100						
	B4	2,252	21.2	1.40	−2.84	17.31		
317.5°	A16	18,040						
	B4	1,300	6.7	3.0	−5.46	16.20		
45°	A16	22,030						
	B4	1,312	7.1	3.40	−5.7	13.33		
45°	A16	33,200						
	B4	2,152	22.3	0.90	−1.96	13.82	0.266	0.256
315°	A16	24,410						
	B4	1,616	22.8	1.16	−2.36	14.83		
315°	A16	12,910						
	B4	804	6.8	3.90	−6.45	13.63		
47.5°	A16	23,410						
	B4	1,420	9.0	2.2	−2.85	13.61		
47.5°	A16	31,580						
	B4	1,864	21.5	1.00	−1.65	13.23	0.280	0.272
312.5°	A16	28,210						
	B4	1,848	20.9	1.30	−1.95	14.68		
312.5°	A16	20,920						
	B4	1,288	9.3	6.7	−7.35	13.80		
50°	A16	19,300						
	B4	1,452	9.3	2.3	−1.94	16.91	0.341	0.334
310°	A16	17,160						
	B4	1,416	8.9	2.8	−2.21	18.51		
52.5°	A16	14,280						
	B4	1,412	9.3	2.4	−1.05	22.1	0.397	0.395
307.5°	A16	12,860						
	B4	1,332	9.0	2.7	−1.09	23.2		
55°	A16	11,760						
	B4	1,492	9.3	2.5	−0.48	29.0	0.452	0.449
305°	A16	16,370						
	B4	2,200	9.0	2.5	−0.48	30.10		
57.5°	A16	9,350						
	B4	1,444	7.0	3.3	−0.070	33.63	0.451	0.451
302.5°	A16	8,452						
	B4	1,360	6.8	3.3	−0.070	37.82		
60°	A16	11,080						
	B4	1,900	9.1	2.5	+0.25	38.23	0.395	0.396
300°	A16	10,130						
		1,788	9.2	2.5	+0.25	39.31		
62.5°	A16	11,620						
	B4	1,540	7.1	3.3	+0.86	30.82	0.269	0.267
297.5°	A16	9,020						
	B4	1,360	6.8	3.3	+0.86	33.93		
65°	A16	9,220						
	B4	872	9.2	2.5	+0.52	21.15	0.106	0.104
295°	A16	14,960						
	B4	980	7.1	3.3	+1.00	14.05		

were calculated from:

$$(P/P_M)_\theta = [(P/P_M)_{15°}\mathfrak{M}(15°)\cot 15°/\mathfrak{M}(\theta)\cot\theta]S(\theta)/S(15°), \quad (1)$$

where $S(\theta)/S(15°)$ is the observed ratio of the number of protons scattered into the rotating counter at the angle θ to the number of protons scattered into the monitor at the angle 15° during the same time interval, divided by a constant factor due to the geometry of the counter apertures. The quantity in brackets is calculated from the tables of $\mathfrak{M}$ in BTE and $(P/P_M)_{15°}$ is the Mott ratio[11] for 15°, calculated from the assumed well parameters $r_0 = e^2/mc^2$ and $D = 10.5$ Mev. These values were taken from unpublished tables furnished us by Professor Breit. If the

[11] The symbols P/P_M and $\mathfrak{R}$ are both used by BTE to represent the Mott ratio.

TABLE IV. *Angular variation of P/P_M at 298 kev. Notation is same as for Table III.*

θ	C	N_P	p	A/p	Corr	R	$(P/P_M)u$	$(P/P_M)c$
15°	*A*4	1,228						
	*B*16	105,296	21.1	1.2	−2.3	10,020	0.881	0.861
345°	*A*4	1,236						
	*B*16	103,296	22.5	1.0	−2.3	9,060		
20°	*A*4	2,972						
	*B*16	41,568	21.1	1.10	−1.67	1,950		
340°	*A*4	3,384						
	*B*16	64,048	21.2	1.10	−1.67	2,050	0.822	0.808
20°	*A*4	4,648						
	*B*16	84,192	23.3	1.00	−1.65	2,120		
20°	*A*4	3,484						
	*B*16	64,304	21.7	1.45	−2.33	2,158		
340°	*A*4	3,176						
	*B*16	53,872	21.7	1.45	−2.33	1,839		
25°	*A*4	4,188						
	*B*16	21,760	23.8	0.99	−1.35	609		
25°	*A*4	5,708						
	*B*16	26,960	21.3	1.7	−1.91	554	0.748	0.737
335°	*A*4	4,440						
	*B*16	23,632	21.3	1.30	−1.34	576		
25°	*A*4	4,788						
	*B*16	24,656	21.1	1.25	−1.11	603		
30°	*A*4	5,340						
	*B*16	8,400	10.0	3.49	−2.34	183.2		
330°	*A*4	4,700						
	*B*16	7,712	9.5	3.49	−2.34	174.0	0.583	0.570
330°	*A*4	4,740						
	*B*16	7,872	21.2	0.85	−1.07	178.7		
30°	*A*4	7,856						
	*B*16	12,112	20.0	1.20	−1.26	165.0		
32.5°	*A*4	4,832						
	*B*16	4,624	20.8	1.60	−1.80	110.5		
32.5°	*A*4	4,220						
	*B*16	3,888	17.1	~1.40	−1.65	106.9	0.516	0.507
327.5°	*A*4	4,880						
	*B*16	4,400	19.3	1.10	−1.42	97.0		
35°	*A*16	6,976						
	*B*4	1,796	10.4	3.49	−4.44	57.2		
35°	*A*16	6,752						
	*B*4	3,244	20.1	1.55	−2.48	56.0	0.401	0.390
325°	*A*16	6,912						
	*B*4	3,432	20.2	1.00	−1.75	53.5		
37.5°	*A*16	15,168						
	*B*4	2,240	21.8	1.30	−3.45	33.0		
37.5°	*A*16	12,432						
	*B*4	1,852	21.2	1.1	−3.05	33.1	0.328	0.319
37.5°	*A*16	11,008						
	*B*4	1,692	16.5	1.30	−3.45	34.3		
322.5°	*A*16	15,568						
	*B*4	2,304	21.3	1.0	−2.85	32.8		
322.5°	*A*16	15,168						
	*B*4	2,092	19.3	1.0	−2.85	30.7		
40°	*A*16	23,360						
	*B*4	1,788	20.6	0.85	−3.68	17.02		
320°	*A*16	23,200						
	*B*4	1,792	23.6	0.75	−3.40	16.97	0.225	0.217
42.5°	*A*16	46,880						
	*B*4	2,044	22.3	0.90	−5.67	9.53		
317.5°	*A*16	41,408						
	*B*4	1,752	23.3	0.775	−5.17	9.21	0.151	0.142
45°	*A*16	24,496						
	*B*4	820	20	1.30	−7.92	7.26		
45°	*A*16	23,760						
	*B*4	728	19.5	1.10	−7.04	6.69		
45°	*A*16	43,712						
	*B*4	1,480	21.4	1.40	−8.36	7.47		
315°	*A*16	36,272						
	*B*4	1,096	15	0.94	−6.33	5.23	0.128	0.118
315°	*A*16	19,264						
	*B*4	700	19	1.30	−7.92	7.87		
315°	*A*16	47,664						
	*B*4	1,420	20.1	1.5	−8.81	7.06		
47.5°	*A*16	27,168						
	*B*4	868	23.0	0.45	−2.76	6.94		
47.5°	*A*16	24,864						
	*B*4	876	21.5	1.20	−4.82	7.72		
312.5°	*A*16	51,888						
	*B*4	2,068	22.5	0.80	−3.72	8.74	0.154	0.148
50°	*A*16	35,392						
	*B*4	1,760	22.3	0.60	−1.78	11.49		
310°	*A*16	39,088						
	*B*4	2,016	22.0	0.83	−2.17	11.35	0.214	0.210
52.5°	*A*16	23,824						
	*B*4	1,680	18.0	1.20	−1.48	15.68		
307.5°	*A*16	18,428						
	*B*4	1,896	19.8	1.25	−1.52	22.70	0.298	0.294
307.5°	*A*16	20,980						
	*B*4	1,644	21.4	1.45	−1.70	17.55		
55°	*A*16	20,096						
	*B*4	2,088	21.2	1.50	−0.680	23.20		
55°	*A*16	20,992						
	*B*4	2,100	21.0	0.70	−0.400	22.21		
305°	*A*16	17,040						
	*B*4	2,016	22.0	0.89	−0.470	26.30	0.364	0.363
57.5°	*A*16	11,344	20.6	1.50	+0.05	41.0		
	*B*4	2,088						
302.5°	*A*16	10,400						
	*B*4	1,836	20.5	1.40	+0.05	39.3	0.494	0.494
60°	*A*16	9,744						
	*B*4	1,544	21.0	1.20	+0.41	35.4		
60°	*A*16	7,974						
	*B*4	2,032	21.5	1.80	+0.68	56.8		
300°	*A*16	9,504						
	*B*4	1,844	20.4	1.30	+0.45	43.2	0.424	0.427
300°	*A*16	16,384						
	*B*4	2,600	21.8	1.35	+0.485	35.5		
65°	*A*16	13,968						
	*B*4	1,620	17.3	1.20	+1.20	25.65		
295°	*A*16	20,736						
	*B*4	1,608	18.5	1.13	+1.13	17.30	0.136	0.138
65°	*A*16	12,880						
	*B*4	1,440	21.9	1.65	+1.65	24.65		
295°	*A*16	22,384						
	*B*4	2,492	21.7	1.65	+1.65	24.65		

corresponding value for the 19.6905-Mev well had been used at 250 kev, for instance, the values of the Mott ratio calculated from our data would only have been 0.42 percent higher throughout at this energy.

Tables III and IV list the angular distribution data obtained for incident proton energies of 249.5 and 298.3 kev. Data were taken at corresponding angles on opposite sides of the beam and averaged. Each run is separately tabulated since these were often taken under different conditions of contamination and pressure in the scattering chamber. The letters *A* and *B* refer to the fixed and rotating counters, respectively, while the numbers 4 and 16 refer to the factor of the scaling circuit used in each case. It will be seen that in both tables the 15° data have the fewest protons on *A*. This is due to the fact that the scattering at 15° is so large that the intensity of the proton beam must be greatly reduced if a reasonable number of protons is to be observed on the rotating counter, which has a very large aperture. This, however, makes the number of protons entering the monitor counter quite small.

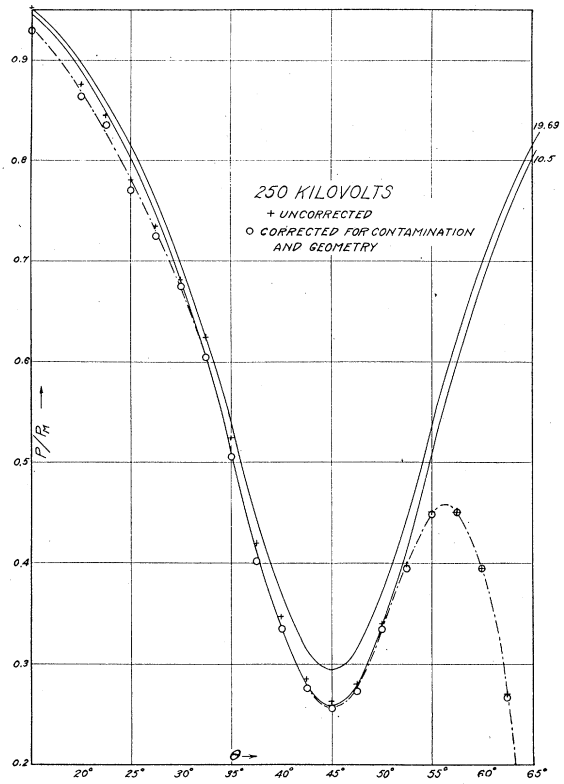

FIG. 10. Proton-proton scattering at 250 kv, second chamber data, plotted as ratio to Mott scattering along with theoretical curves (solid lines) for $r_0=\frac{3}{4}e^2/mc^2$, $D=19.6905$ Mev (upper curve) and $r_0=e^2/mc^2$, $D=10.500$ Mev (lower curve). The dashed curve is experimental for a proton energy of 249.5 kev at the scattering volume; its value at the higher angles yields the efficiency correction curve, Fig. 4.

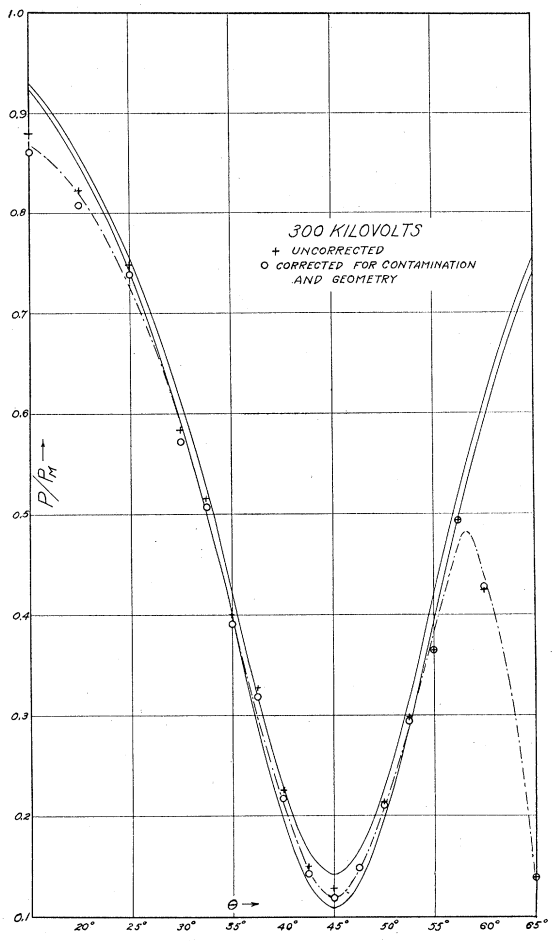

FIG. 11. Proton-proton scattering at 300 kv, second chamber data, plotted as ratio to Mott scattering along with theoretical curves (solid lines) for $r_0=\frac{3}{4}e^2/mc^2$, $D=19.6905$ Mev, and $r_0=e^2/mc^2$, $D=10.500$ Mev. The dashed curve is experimental, for a proton energy of 298.3 kev at the scattering volume.

These data are again presented in Figs. 10 and 11, while Figs. 5 and 6 show the corresponding correction curves. The experimental voltages are slightly lower than those for the theoretical curves. This would be of greatest importance at 45°, where the theoretical curve for 298.3 kev (the experimental value) would be 2 percent higher and account for part of the discrepancy.

In Table V are listed the data on the energy variation of P/P_M for 45°, shown also in Fig. 12. Figures 4 and 7 show the corrections for these data. The angle 45° was chosen because, as is seen, the anomaly is large and the choice between potential wells is here most easily made. Because of the stopping power of the gas in the scattering chamber, the energy of the protons when scattered was less than the energy given by the accelerating voltage. Livingston and Bethe's[12] curves for the stopping cross section of protons in air, together with the relative stopping power of hydrogen were used to correct for this. The total path length of the protons in hydrogen at the oil manometer pressure was assumed to be 12 cm. This corresponds to assuming that one-half of the length of the differential pumping system capillary has hydrogen at manometer pressure in it. The corrections amount to 3.46 kev/mm of mercury at 175 kev and 2.86 kev/mm of mercury at 325 kev. In taking the data, it was attempted to set the accelerating voltage higher by the correct amount, but since this was

[12] M. S. Livingston and H. A. Bethe, Rev. Mod. Phys. 9, 245 (1937).

not always successful, the energies at the scattering volume were individually calculated.

It may be seen that at 15°, Eq. (1) should reduce to the identity $(P/P_M)_{15°}=(P/P_M)_{15°}$. However, the 15° points in the angular distributions, Figs. 10 and 11, do not fall on the proper theoretical curves. This is a manifestation of error in the small angle data. There were a number of experimental difficulties encountered at small angles which may have caused error. (1) It was possible to monitor only on one side of the beam. (2) The beam struck the body of the counter. This caused no increase in scattering when the chamber was evacuated, but the possible effect of the presence of the gas is unknown. (3) Because of the difference in the geometries of the monitors and the rotating counter, very small beam currents had to be used. As seen in the tables, the statistical accuracy of the counting rate in the monitor counters is poor. Also, it is possible that the necessary changes in the probe and focusing voltages may have introduced a slight shift in beam direction and changed the intensity distribution within the beam itself. (4) The geometry correction is largest at small angles. (5) An error in the geometrical factor for the counters would be most noticeable at small angles. (6) No corrections have been made for finite beam width. These are estimated in BTE, p. 1040, are largest at small angles, and increase the P/P_M ratio. (7) No corrections have been made for multiple scattering effects. (8) The divided circle and vernier may have been inaccurate.

In order to try to find which of these sources of error existed, data were taken as a function of scattering chamber pressure. A smaller slit was used on the rotating counter to reduce its counting rate. A minimum of about 5 percent in the scattering yield at 20° for both 250 kv and 300 kv was observed at about 12 mm of oil pressure. The values at oil pressures below 8 mm approach the theoretical yield within 1 percent, but the statistical accuracy of the low pressure data is not that good. However, some of our scattering data were taken in the pressure range which we subsequently found to be a minimum. An effect seems to be present at 15°, but it is of smaller magnitude and the statistical accuracy of the points is not good, so that no conclusions can be drawn for this angle. No pressure effect was found at 35°.

Our apparatus was of course not designed to measure a pressure effect, and no account has been taken of this effect in either the tabulated data or the curves. Attempts to interpret it, however, have suggested a number of factors which may be valuable in criticizing our data. It is interesting that the greatest effect of pressure variation occurred near the transition between laminary and molecular flow of the gas leaving the capillary. A pressure effect would of course suggest multiple scattering, which would be more likely to reduce our P/P_M ratios than to increase them. The 15° monitoring counter, whose yield goes into the denominator of the fraction P/P_M, would be expected to receive the greatest multiple scattering effect. Finally, there is an important difference between the two scattering chambers used in these experiments. In the first chamber the two counters involved were the same distance from the scattering volume, but

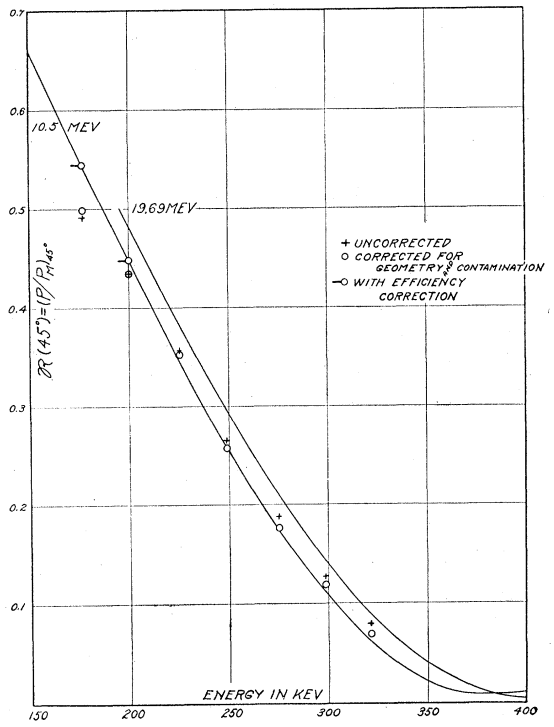

FIG. 12. Proton-proton scattering at 45°, second chamber data, plotted as ratio to Mott scattering along with theoretical curves (solid lines) for $r_0=\frac{3}{4}e^2/mc^2$, $D=19.6905$ Mev, and $r_0=e^2/mc^2$, $D=10.500$ Mev.

TABLE V. *Energy variation of* $(P/P_M)_{45°}$. *Notation is same as for Table III except: E, proton energy in kev;* $(P/P_M)e$, *ratio to Mott with geometry, contamination and efficiency corrections.*

E	C	N_P	θ	p	A/p	Corr	R	$(P/P_M)u$	$(P/P_M)c$	$(P/P_M)e$
	$A16$	22,080								
	$B4$	2,400	45.0°	23.0	0.82	+0.062	24.38	0.495	0.498	0.544
176.5	$A16$	25,504								
	$B4$	2,912	315.0°		0.83		25.5			
	$A16$	19,328								
	$B4$	1,952	45.0°	22.4	0.80	−0.30	22.5	0.435	0.434	0.448
200.2	$A16$	19,968								
	$B4$	2,000	315.0°	22.5	0.80		22.62			
	$A16$	25,184								
	$B4$	2,072	45.0°	23.0	0.95	−1.022	18.42	0.357	0.353	0.353
225.9	$A16$	26,640								
	$B4$	2,204	315.0°	23.0			18.52			
	$A16$	22,048								
	$B4$	1,312	45.0°	7.1	3.4	−5.7	13.33	0.251		
	$A16$	33,200								
	$B4$	2,052	45.0°	22.3	0.90	−1.96	13.82	0.261	0.256	0.256
249.5	$A16$	20,656								
	$B4$	1,288	315.0°	7.1	3.9	−6.45	13.96	0.263		
	$A16$	24,448								
	$B4$	1,616	315.0°	23.2	1.16	−2.36	14.83	0.279		
	$A16$	34,768								
	$B4$	1,624	45.0°	21.8	2.0	−6.35	10.45	0.193	0.177	0.177
275.3	$A16$	43,648								
	$B4$	1,924	315.0°	21.5	1.50	−4.98	9.88	0.183		
	$A16$	24,496								
	$B4$	820	45.0°	20.0	1.30	−7.92	7.26			
	$A16$	23,760								
	$B4$	728	45.0°	19.5	1.10	−7.04	6.69			
	$A16$	43,712								
	$B4$	1,480	45.0°	21.4	1.40	−8.36	7.47	0.128	0.118	0.118
298.3	$A16$	36,272								
	$B4$	1,096	315.0°	15.0	0.94	−6.33	5.23			
	$A16$	19,264								
	$B4$	700	315.0°	19.0	1.30	−7.92	7.87			
	$A16$	47,664								
	$B4$	1,420	315.0°	20.1	1.50	−8.81	7.06			
	$A16$	42,928								
	$B4$	888	45.0°	24.0	1.13	−13.9	4.42	0.081	0.0703	0.0703
321.4	$A16$	38,672								
	$B4$	832	315.0°	24.0	1.13		4.62			

in the second chamber they are at quite different distances. It would seem that any pressure effect that may exist at 15° should find its origin in this difference of distances, and it may be that multiple scattering could thus affect the monitor and rotating counters differently.

Unfortunately, time limitations prevented a more thorough investigation of this source of error. Nevertheless, other experimental errors, particularly in the divided circle, statistics, the geometrical factor, and pick-up from sparks at the higher voltages, can account for the deviations between the experimental data and the theoretical scattering curves for a potential well of e^2/mc^2 radius and 10.500-Mev depth. All of the data, taken as a function of energy with two different scattering chambers, and also as a function of angle are in consistent agreement with calculations based on this interaction potential well.

The authors are greatly indebted to Professor G. Breit for encouraging discussions of many aspects of this problem and for the use of the tabulated theoretical results. They have also benefitted by discussions with Professor R. G. Herb. They wish to express their gratitude to Mr. J. P. Foerst for his kind cooperation and the accurate construction of the scattering chambers, and to the Wisconsin Alumni Research Foundation for financial support.